Electronic Supplementary Material (ESI) for Dalton Transactions.
This journal is © The Royal Society of Chemistry 2019

Electronic Supporting Information for

Revisiting the Reactivity of Tetrachloroauric acid with *N,N*-Bidentate Ligands: Structural, Molecular, and Spectroscopic Insights.

R. Tyler Mertens, Jong Hyun Kim, Will C. Jennings, Sean Parkin, and Samuel G. Awuah*

Department of Chemistry, University of Kentucky, Lexington Kentucky 40506, United States

Correspondence to: awuah@uky.edu

Contents

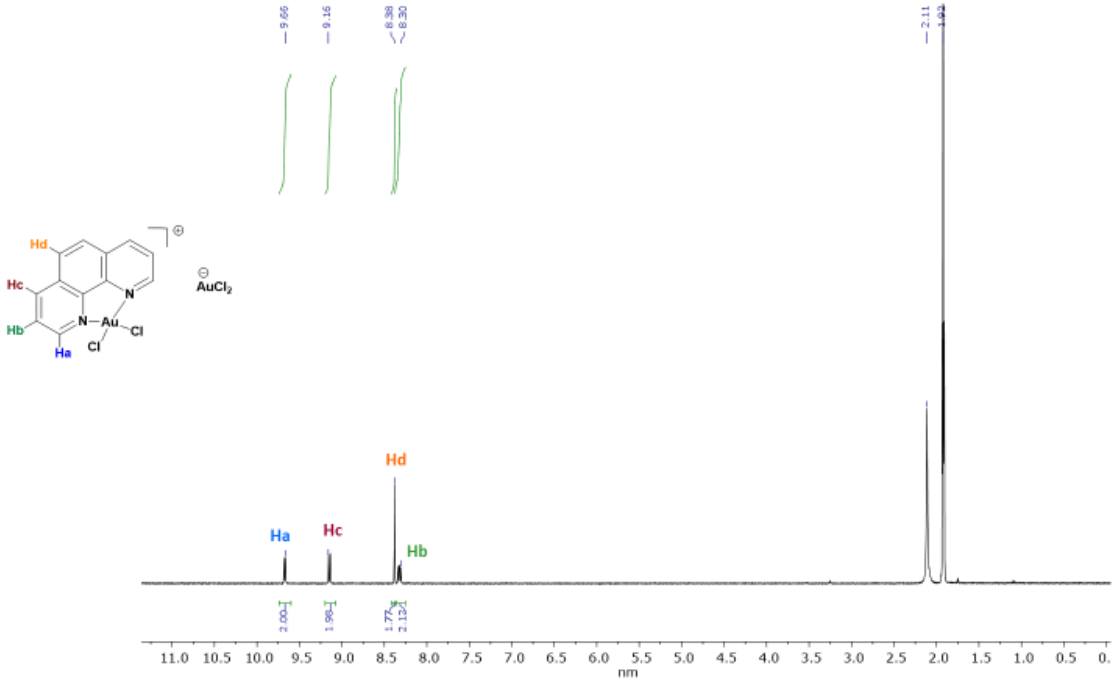

Figure S1. ^{1}H NMR [Au(phen)Cl$_2$][AuCl$_2$] (1) (400 MHz, MeCN-*d*$_3$)

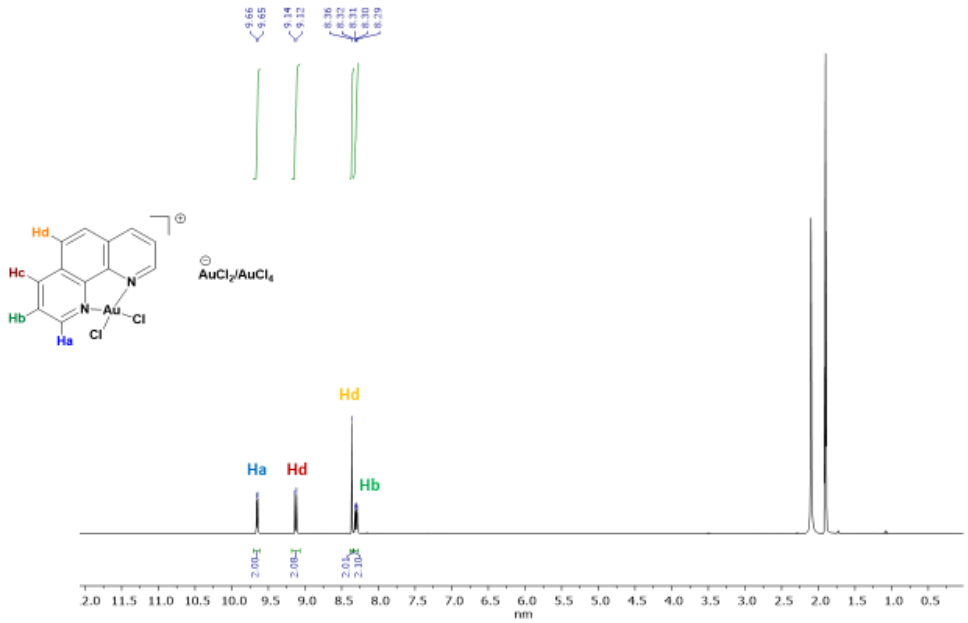

Figure S2. ^{1}H NMR [Au(phen)Cl$_2$][AuCl$_4$][AuCl$_2$] (2) (400 MHz, MeCN-*d*$_3$)

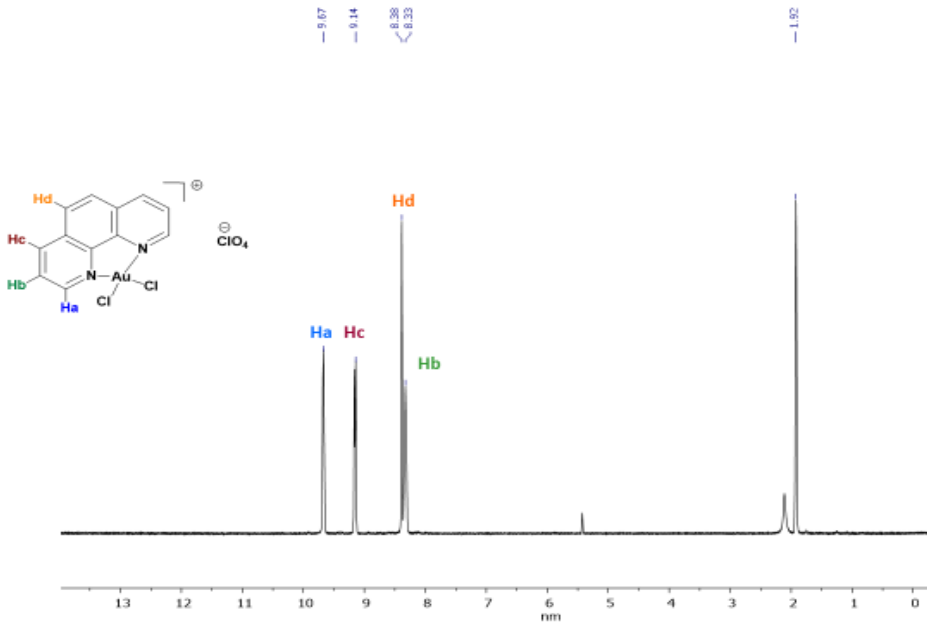

Figure S3. ^{1}H NMR [Au(phen)Cl$_2$][ClO$_4$] (3) 400 MHz, MeCN-*d*$_3$)

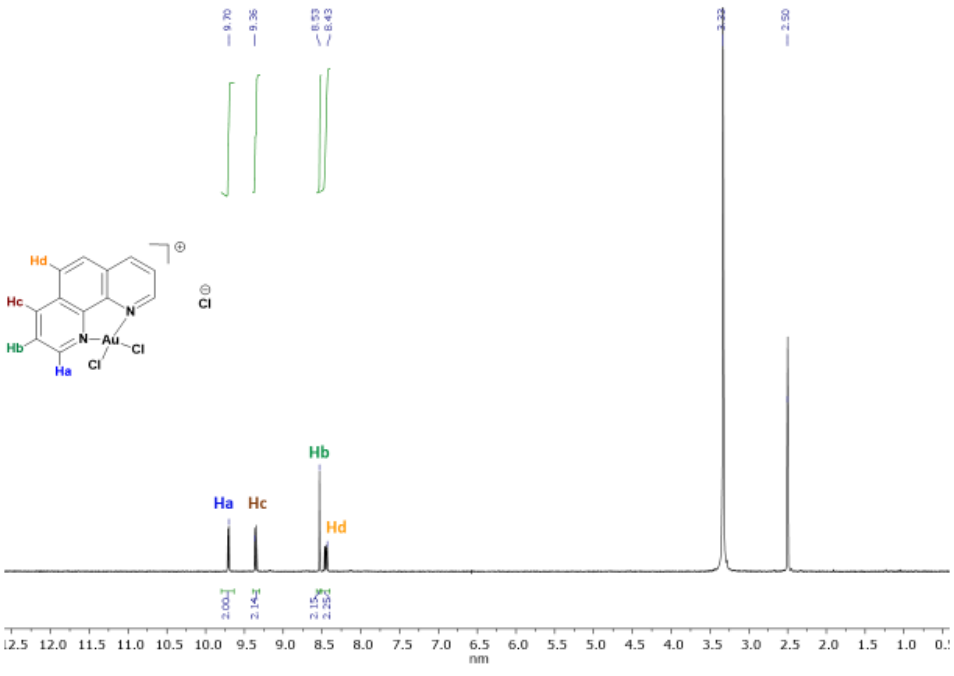

Figure S4. ^{1}H NMR [Au(phen)Cl$_2$][Cl] (4) (400 MHz, DMSO-*d*$_6$)

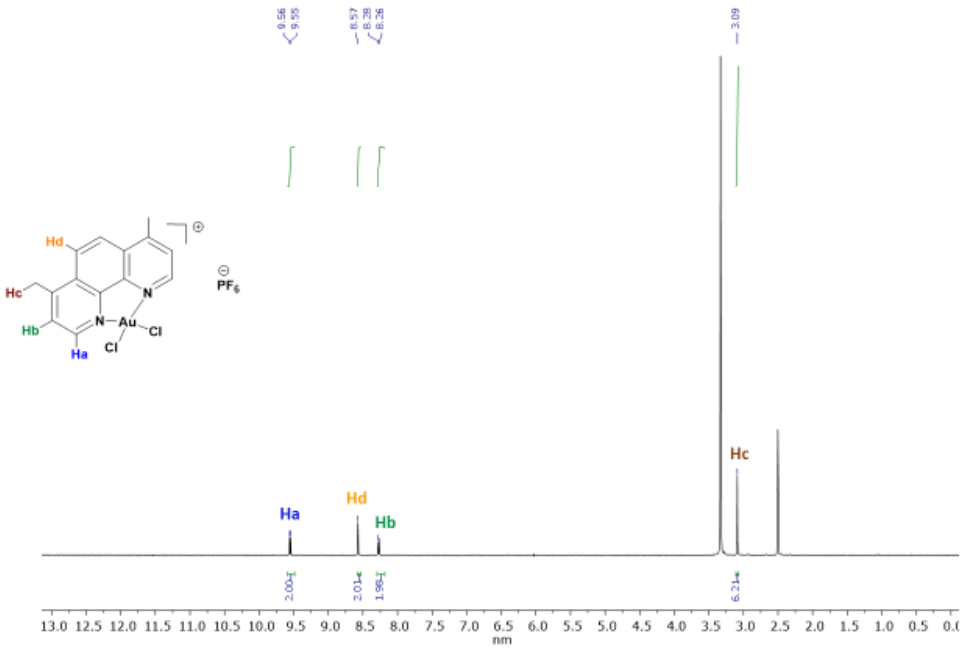

Figure S5. ^{1}H NMR [Au(4,7-dmp)Cl$_2$][PF$_6$] (5) (400 MHz, DMSO-*d*$_6$)

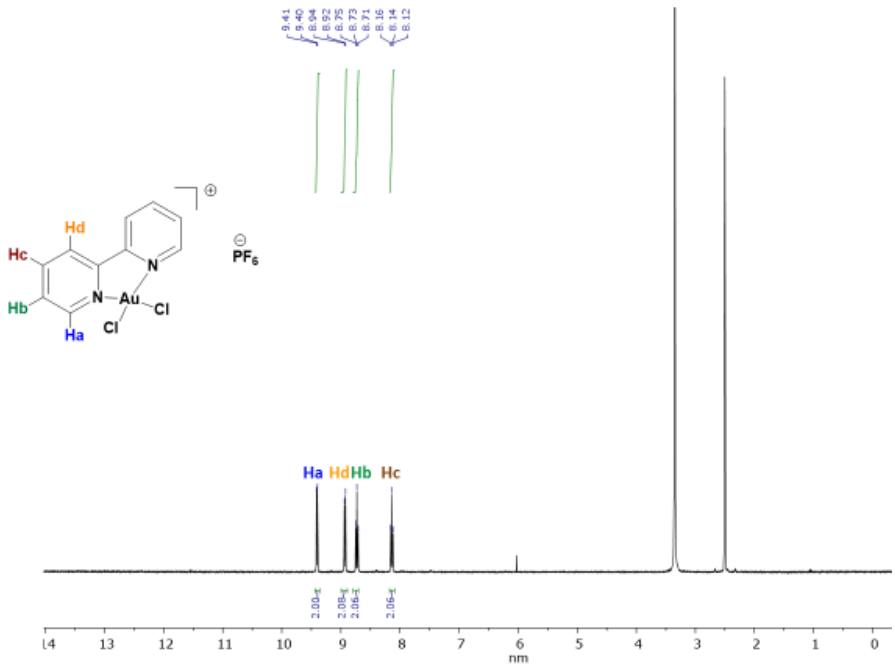

Figure S6. ^{1}H NMR [Au(bpy)Cl$_2$][PF$_6$] (6) (400 MHz, DMSO-*d*$_6$)

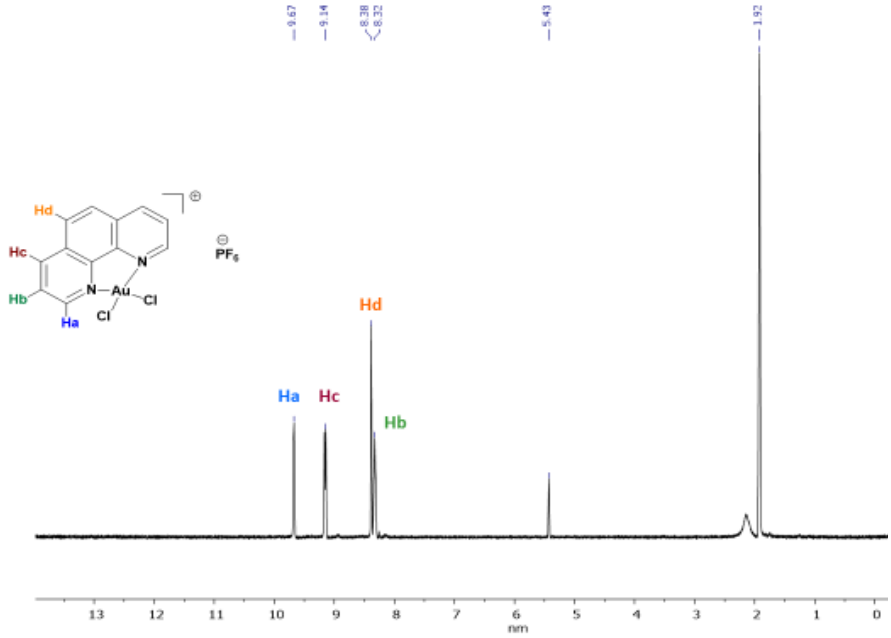

Figure S7. ^{1}H NMR [Au(phen)Cl$_2$][PF$_6$] (7) (400 MHz, MeCN-*d*$_3$)

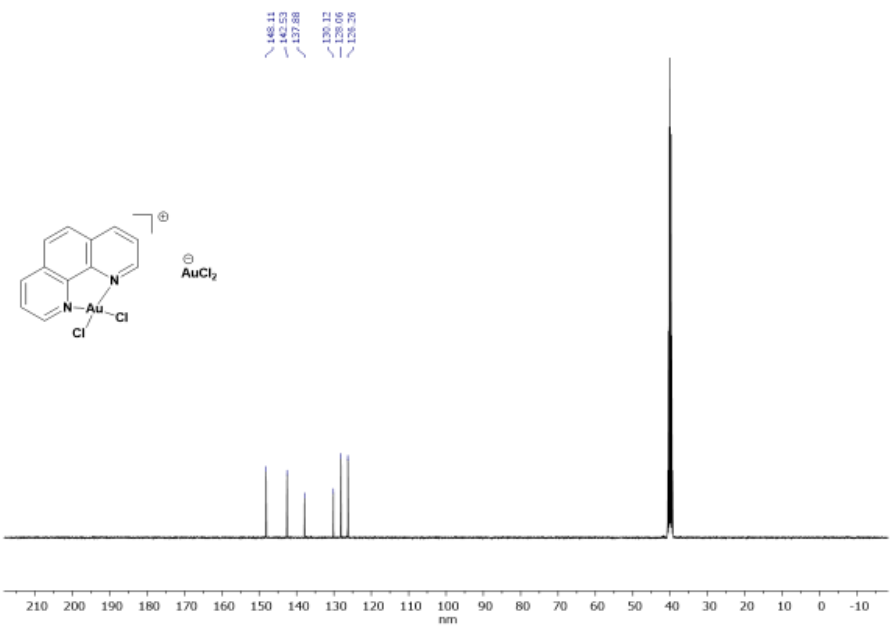

Figure S8. ^{13}C{H} NMR [Au(phen)Cl$_2$][AuCl$_2$] (1) (400 MHz, DMSO-*d*$_6$)

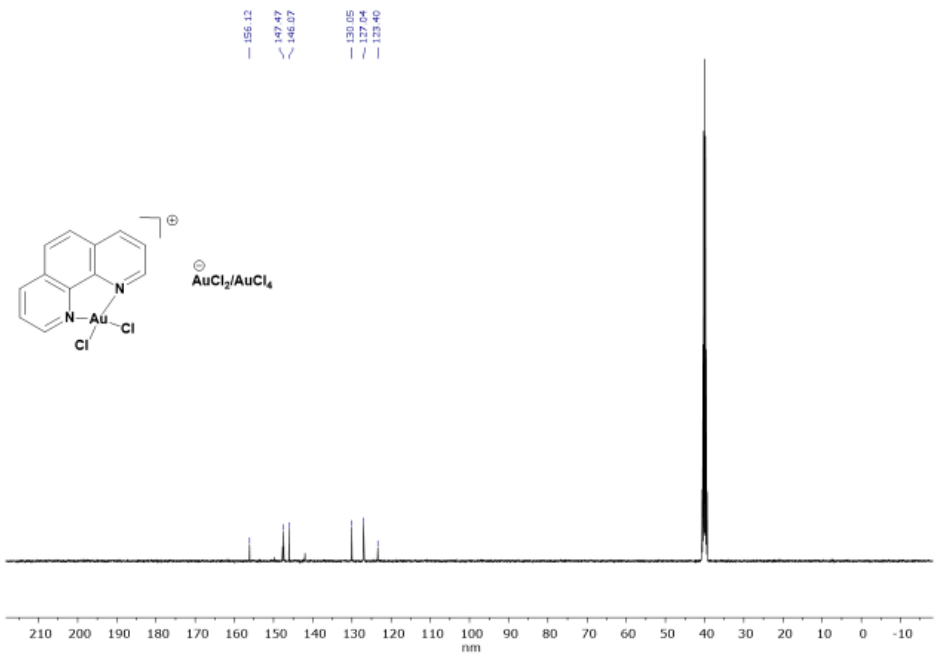

Figure S9. $^{13}C\{H\}$ NMR [Au(phen)Cl_2][$AuCl_4$][$AuCl_2$] (2) (400 MHz, DMSO-d_6)

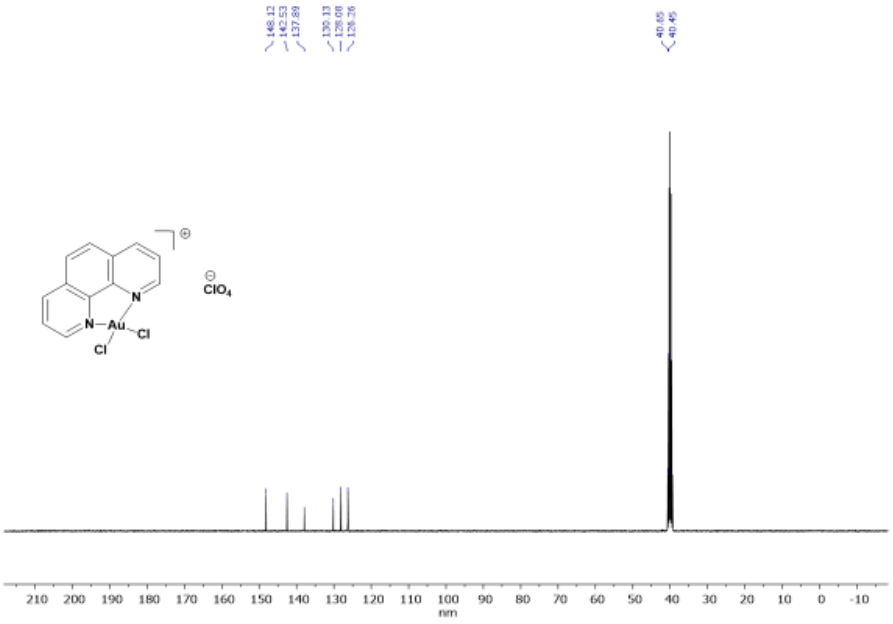

Figure S10. $^{13}C\{H\}$ NMR [Au(phen)Cl_2][ClO_4] (3) (400 MHz, DMSO-d_6)

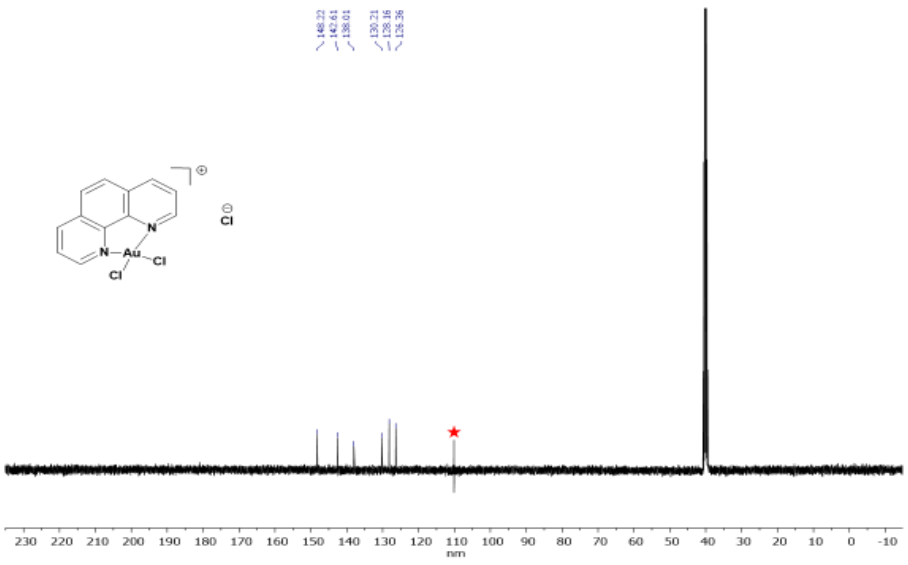

Figure S11. **^{13}C{H} NMR [Au(phen)Cl$_2$][Cl] (4)** (400 MHz, DMSO-d_6). * mechanical noise.

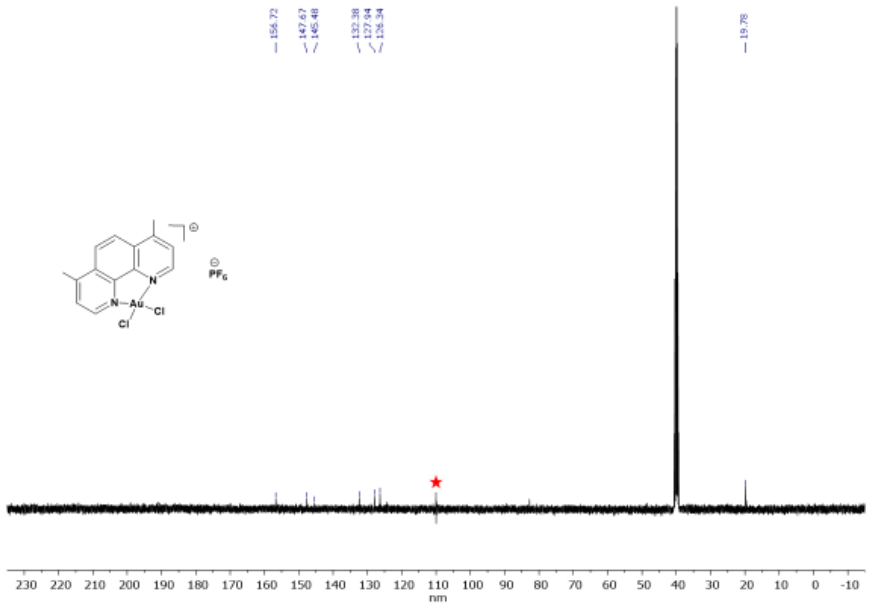

Figure S12. **^{13}C{H} NMR [Au(4,7-dmp)Cl$_2$][PF$_6$] (5)** (400 MHz, DMSO-d_6). * mechanical noise

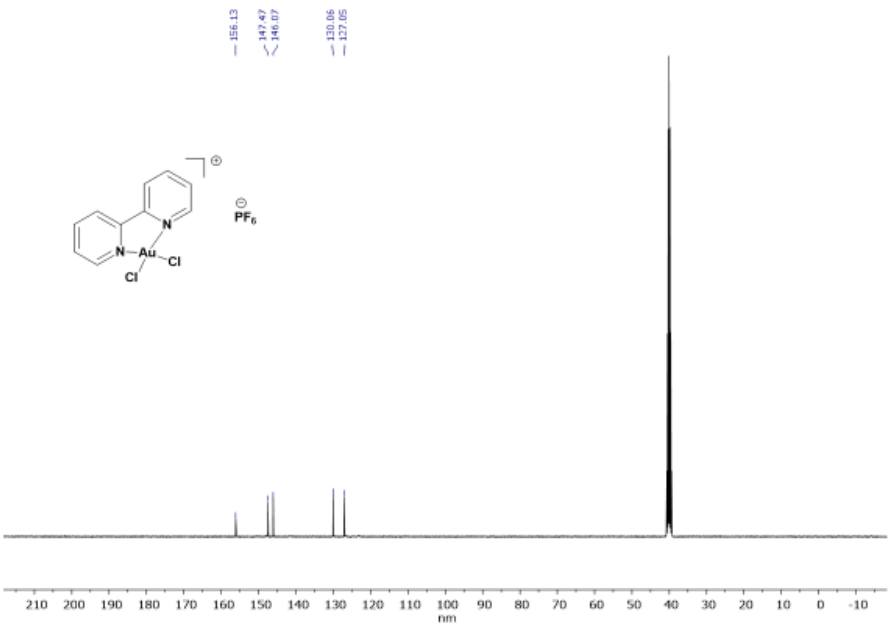

Figure S13. $^{13}C\{H\}$ **NMR [Au(bpy)Cl$_2$][PF$_6$] (6)** (400 MHz, DMSO-d_6)

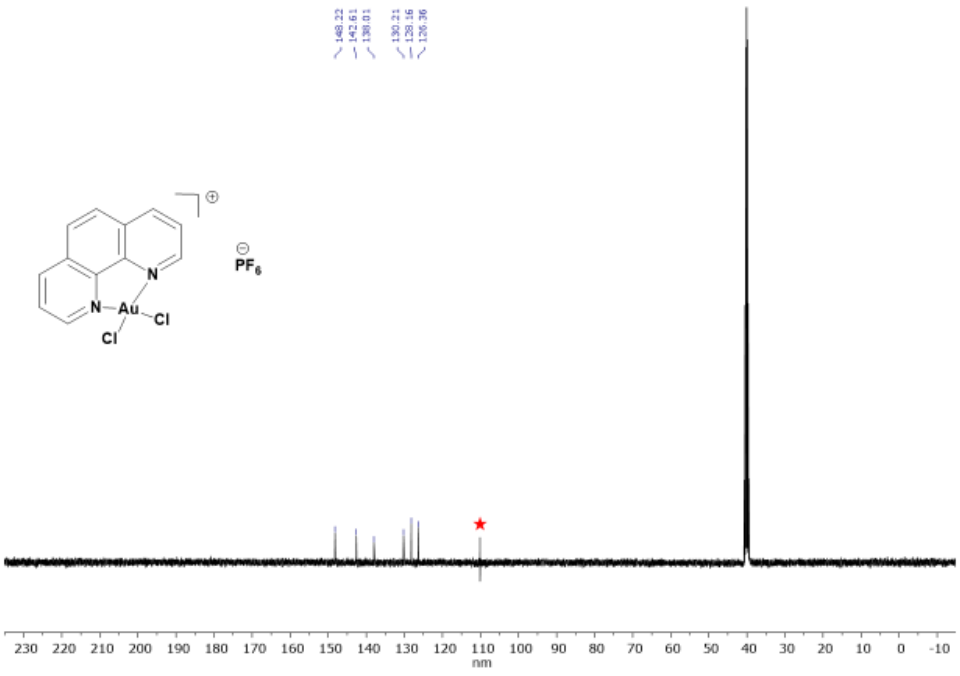

Figure S14. $^{13}C\{H\}$ **NMR [Au(phen)Cl$_2$][PF$_6$] (7)** (400 MHz, DMSO-d_6). * mechanical noise

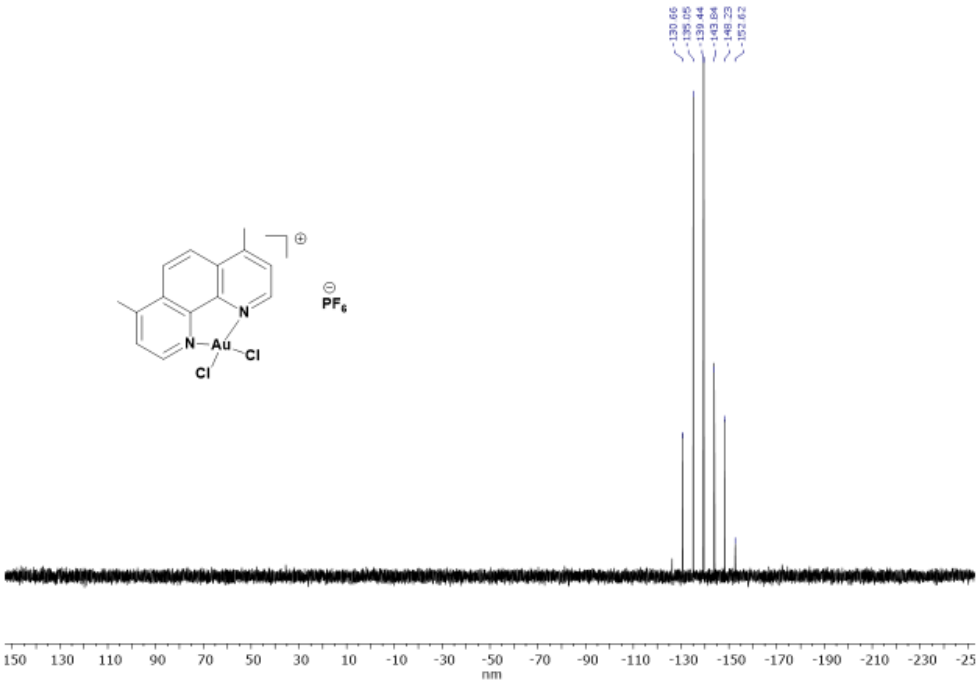

Figure S15. ^{31}P{H} NMR [Au(4,7-dmp)Cl$_2$][PF$_6$] (5) (400 MHz, DMSO-*d*$_6$)

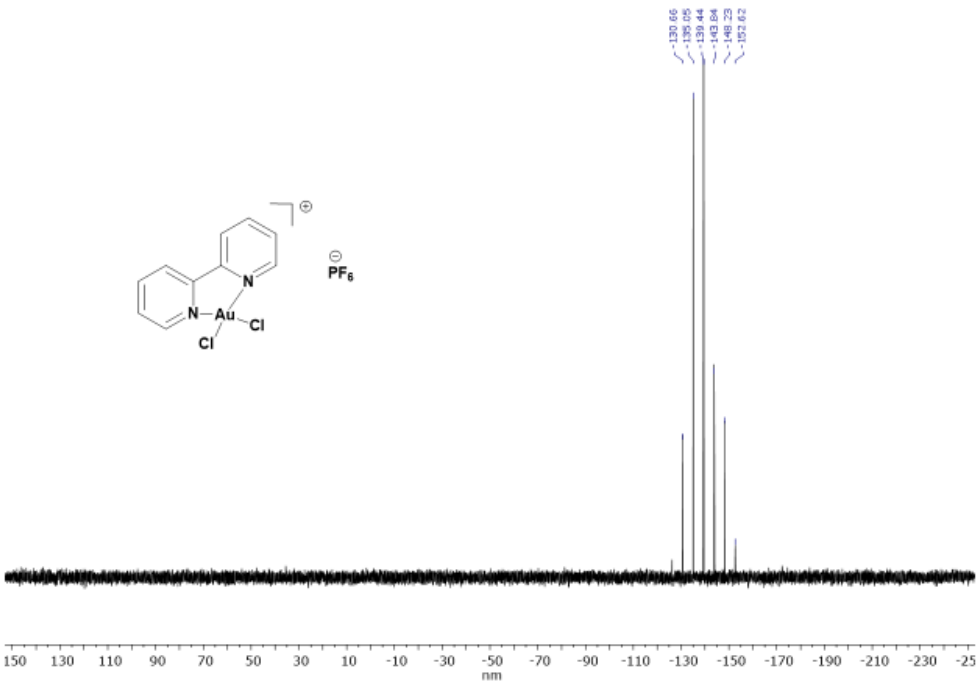

Figure S16. ^{31}P{H} NMR [Au(bpy)Cl$_2$][PF$_6$] (6) (400 MHz, DMSO-*d*$_6$)

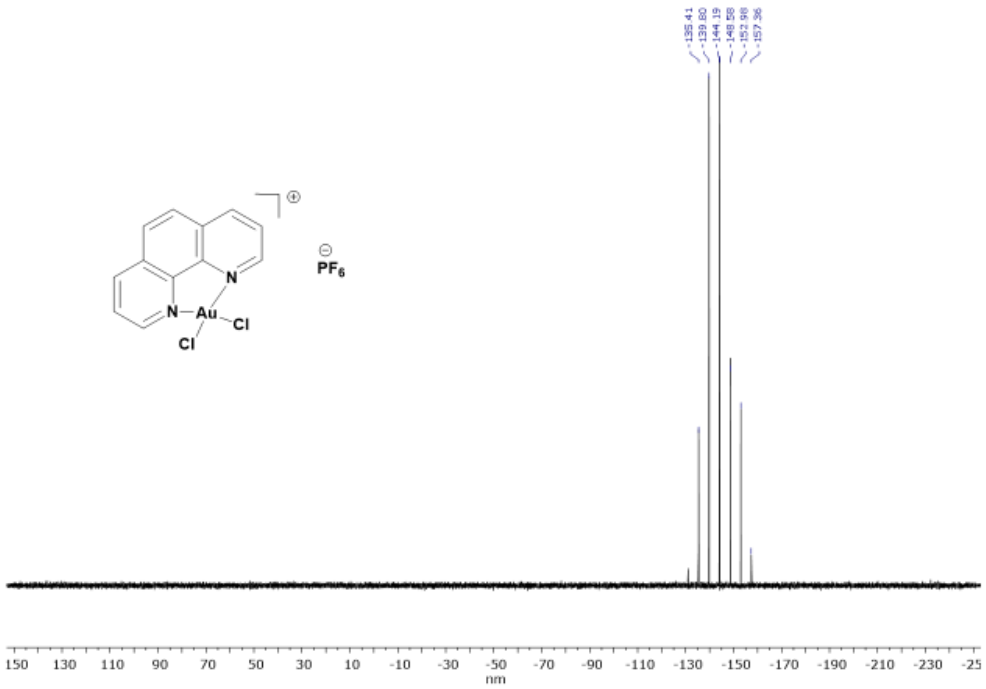

Figure S17. $^{31}P\{H\}$ NMR [Au(phen)Cl_2][PF_6] (7) (400 MHz, DMSO-d_6)

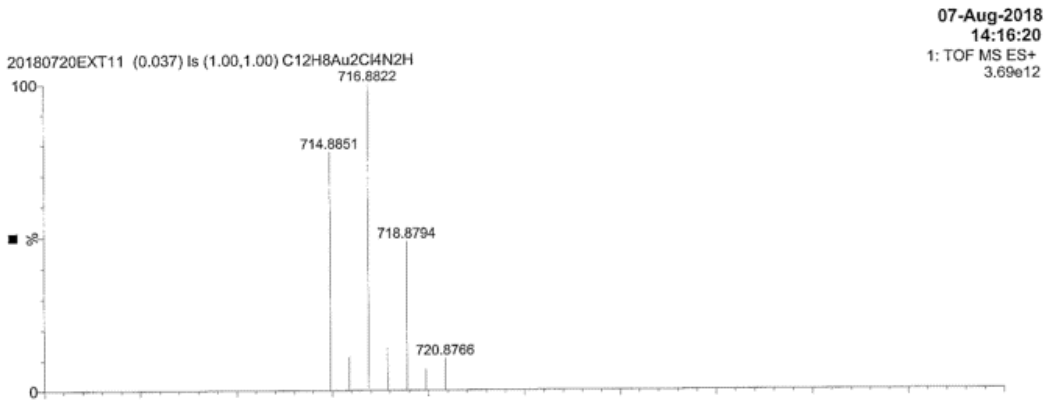

Figure S18. MS (m/z, EI HRMS) [M+H[[Au(phen)Cl_2][$AuCl_2$] (1)

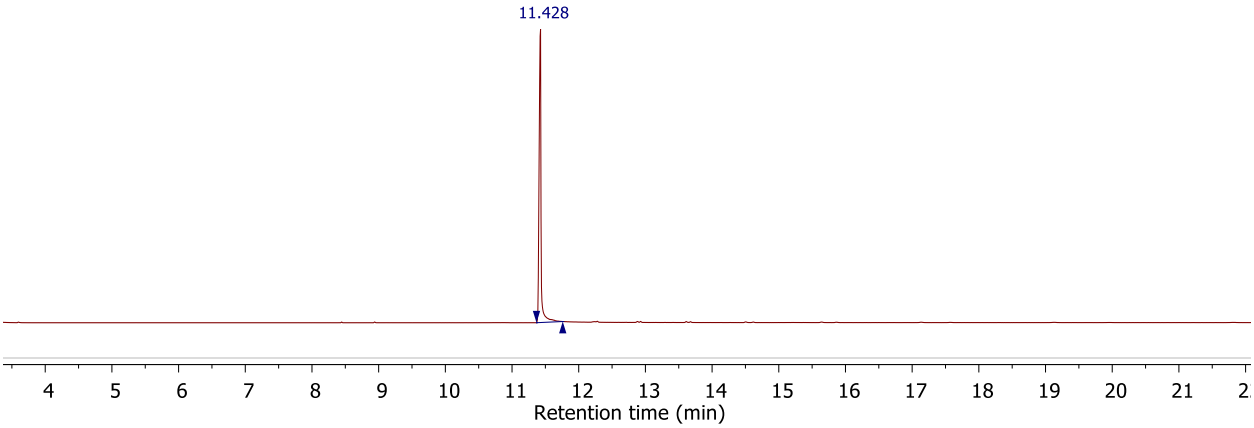

Figure S19. Retention time of GC-MS of the filtrate of reaction to generate compound **1**.

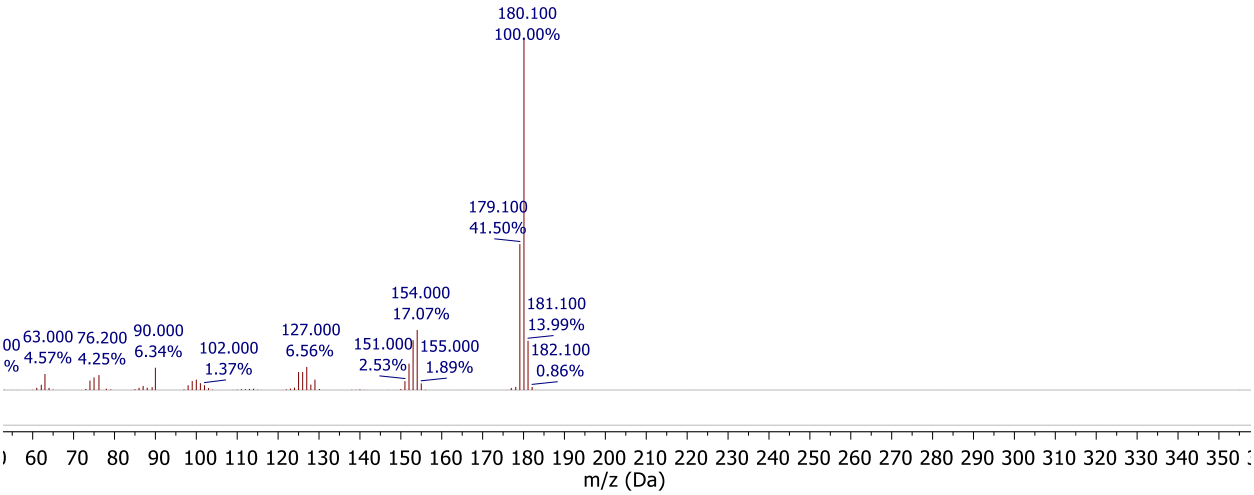

Figure S20. m/z of the filtrate of reaction to generate compound **1** corresponds to free phenanthroline.

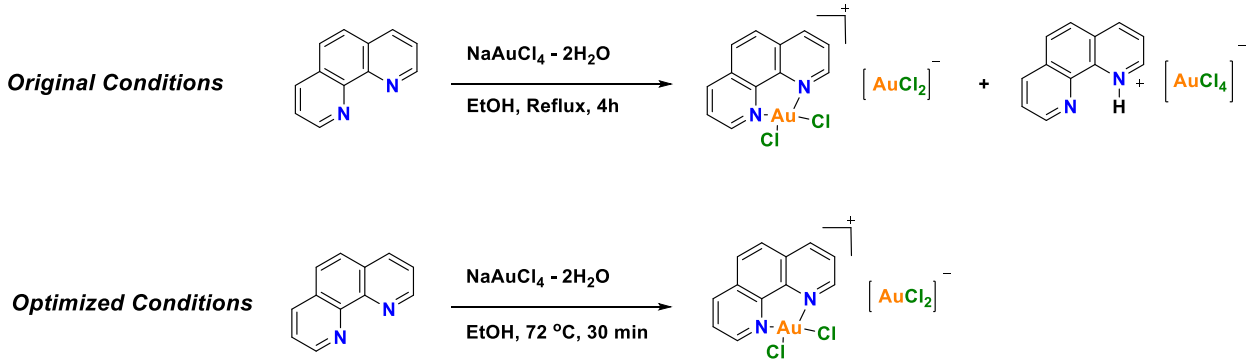

Figure S21. Reactions of $NaAuCl_4.2H_2O$ with phenanthroline. *For each reaction, an equimolar mixture of $NaAuCl_4.2H_2O$ and phenanthroline were added together in 10 mL of ethanol. The reactions were subjected to the conditions mentioned above in the reaction scheme. The solid was collected, washed with ether, and vacuum dried in air. ^{1}H NMR spectra were taken in DMSO-d_6.

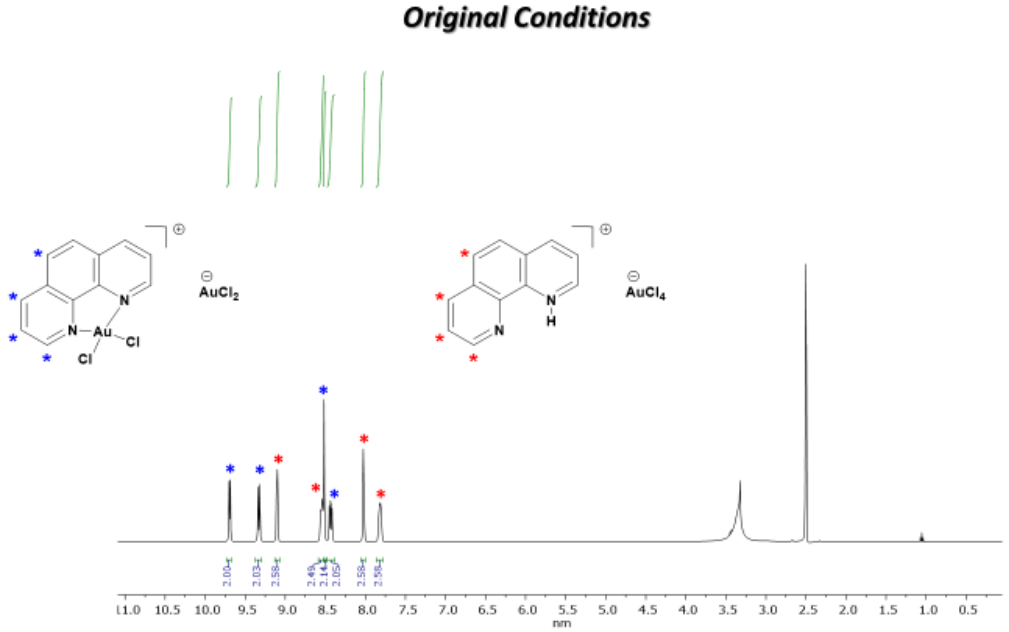

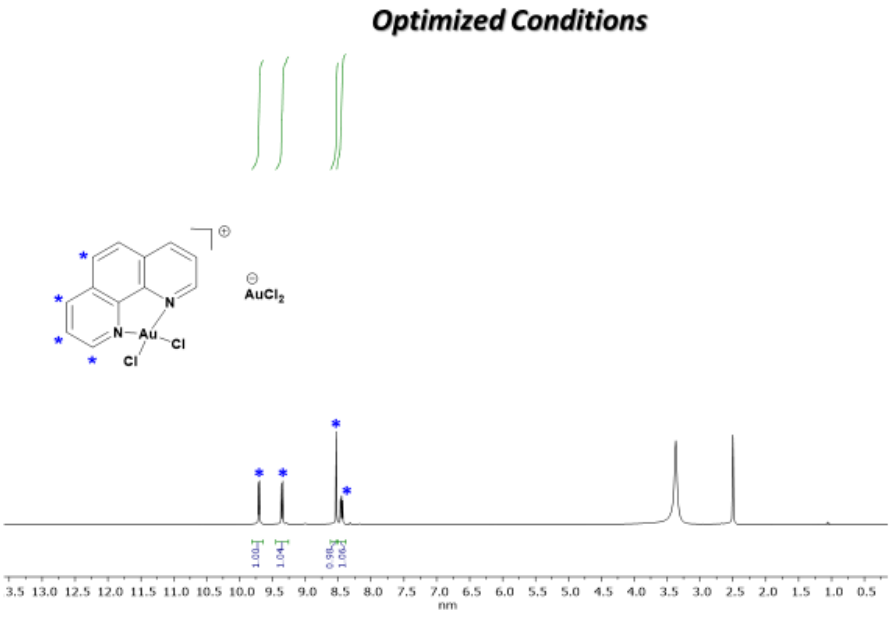

Figure S22. ^{1}H NMR of isolated complexes following the reactions of $NaAuCl_4.2H_2O$ with phenanthroline under original conditions or our optimized condition.

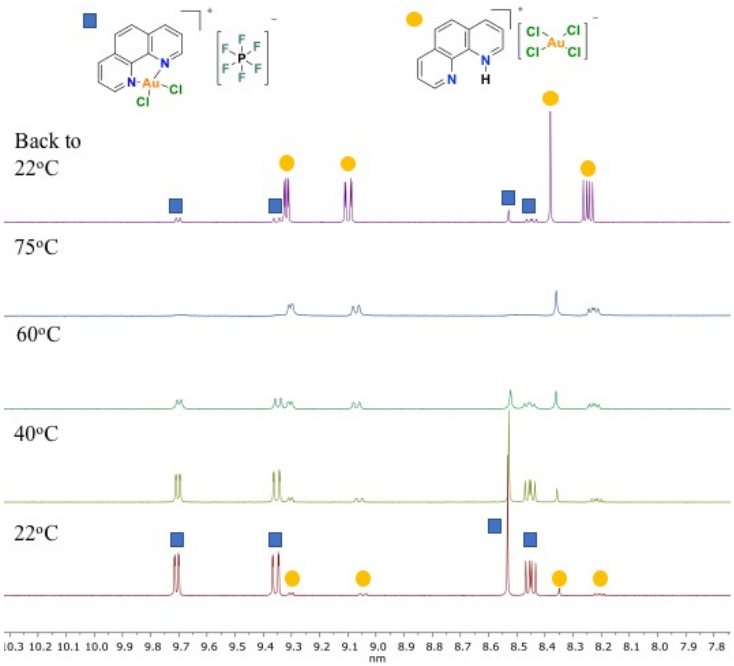

Figure S23: VT H^{1} NMR study of **7** at temperatures 22 °C, 40 °C, 60 °C, 75 °C, followed by a scan once cooled back to 22 °C.

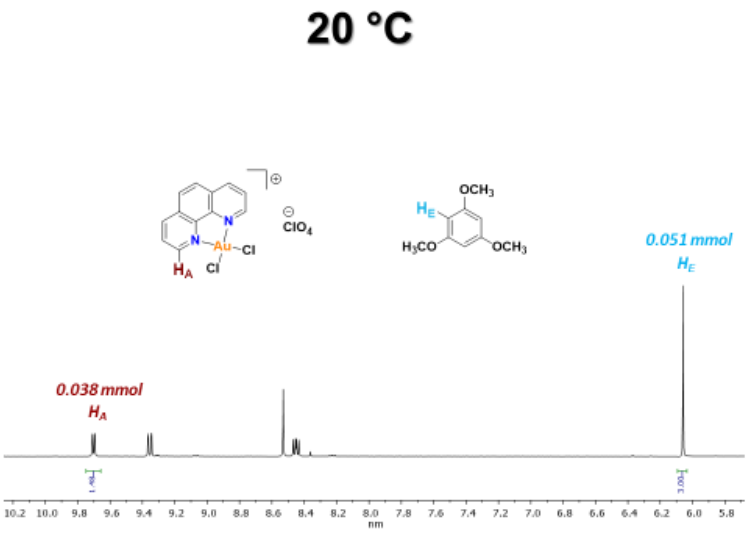

Figure S24. Q-VT-^{1}H NMR at 20 °C in DMSO-d_6.

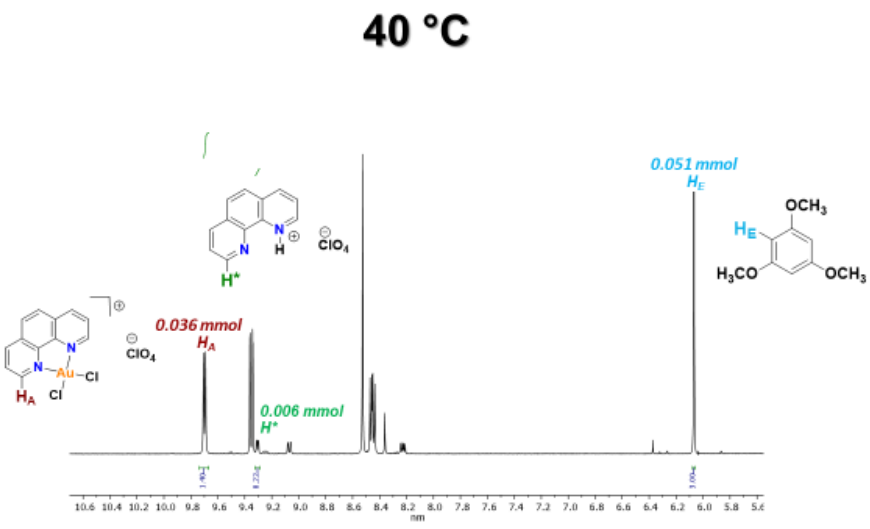

Figure S25. Q-VT-^{1}H NMR at 40 °C in DMSO-d_6.

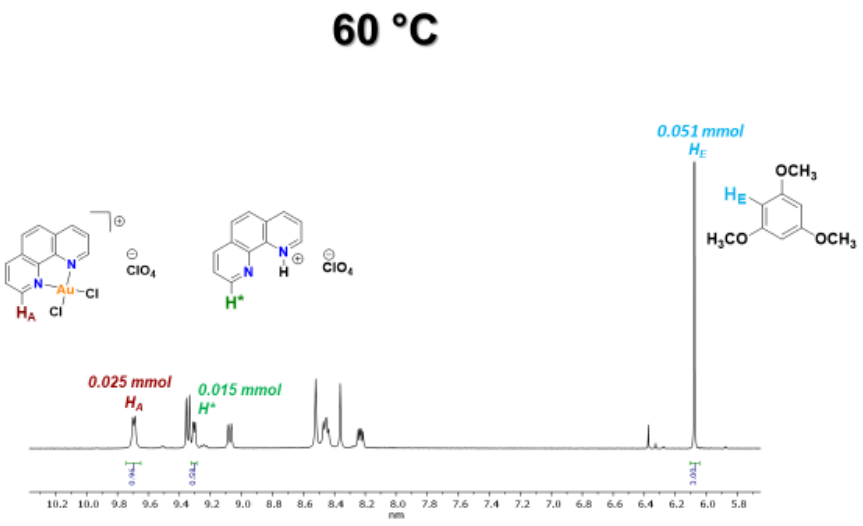

Figure S26. Q-VT-^{1}H NMR at 60 °C in DMSO-d_6.

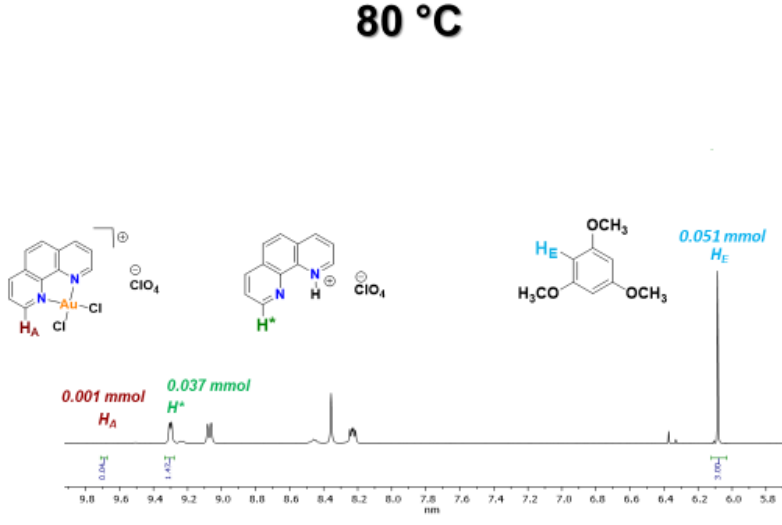

Figure S27. Q-VT-^{1}H NMR at 80 °C in DMSO-d_6

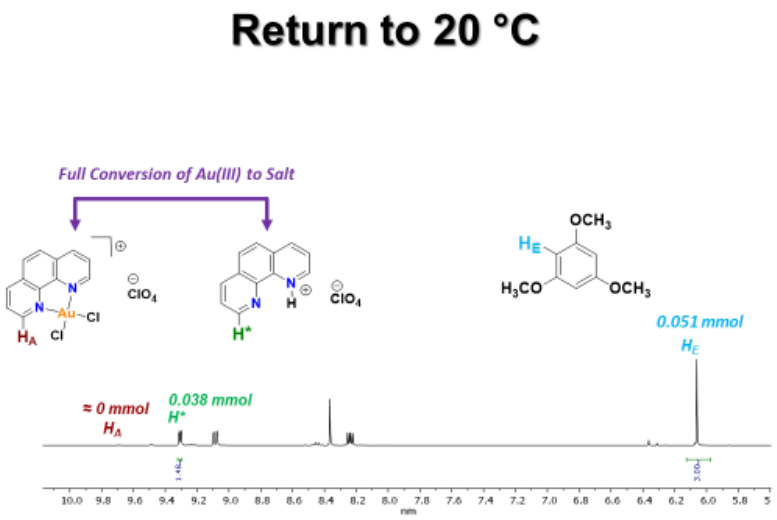

Figure S28. Q-VT-^{1}H NMR at 20 °C in DMSO-d_6.

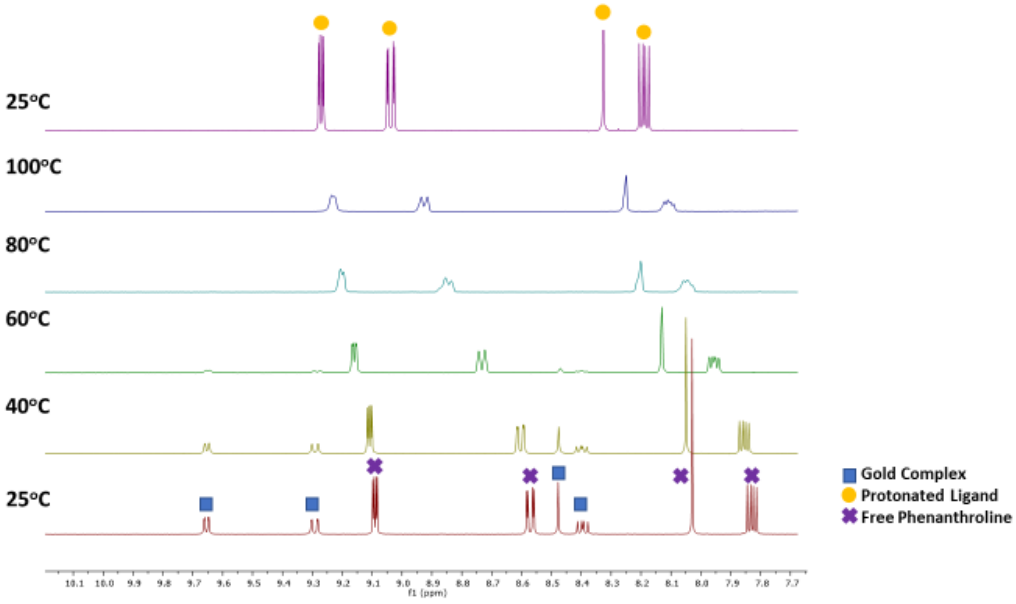

Figure S29: Variable temperature ^{1}H NMR (400 MHz) of complex **(3)** with free phenanthroline as the starting impurity. Temperature increase shows conversion of both materials to the protonated ligand.

Table S1. X-ray crystal structures of gold(III) complexes under investigation

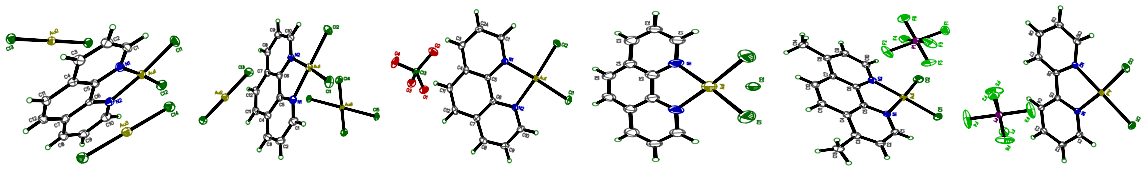

	1	2	3	4	5	6
Crystal Data						
Chemical Formula	$C_{12}H_8Au_2Cl_4N_2$	$C_{12}H_8Au_2Cl_5N_2$	$C_{12}H_8AuCl_3N_2O_4$	$C_{12}H_8AuCl_3N_2$	$C_{14}H_{12}AuCl_2F_6N_2P$	$C_{10}H_8AuCl_2F_6N_2P$
M_r	715.94	751.39	547.52	483.52	621.10	569.02
Crystal System	Triclinic	Triclinic	Orthorhombic	Orthorhombic	Monoclinic	Monoclinic
Space Group	$P\bar{1}$	$P\bar{1}$	*Pbca*	*Cmcm*	$P2_1/n$	$P2_1/n$
Temperature (K)	90	90	90	90	90	90
a, *b*, *c* (Å)	7.3559(2) 7.9171(2) 13.8613(4)	7.4092(2) 7.7822(2) 14.3986(3)	15.2841(3) 12.1249(3) 15.5256(3)	11.2927(17) 17.827(3) 6.4414(8)	7.0330(2) 14.1302(1) 17.3904(4)	6.8269(1) 14.7624(3) 14.6209(3)
α, β, γ (°)	74.929(1) 77.645(1) 84.574(1)	84.463(1) 77.729(1) 87.429(1)	90 90 90	90 90 90	90 93.714(1) 90	90 100.956(1) 90
V (Å)	760.78(4)	807.22(3)	2877.18(11)	1296.8(3)	1724.59(7)	1416.08(5)
Density (g/cm^3)	3.125	3.091	2.528	2.477	2.392	2.669
Z	2	2	8	4	4	4
Radiation Type	Mo Kα	Mo Kα	Mo Kα	Mo Kα	Mo Kα	Mo Kα
μ (mm^{-1})	19.952	18.972	10.801	11.942	8.995	10.841
F(000)	640.0	674.0	2048.0	896.0	1168.0	1056
Data Collection						
Absorption Correction	Multi-Scan	Multi-Scan	Multi-Scan	Multi-Scan	Multi-Scan	Multi-Scan
Number of Reflections	3472	3691	3302	864	3940	3238
T_{min}	0.397	0.477	0.465	0.569		
T_{max}	0.563	0.563	0.563	0.699	0.450	0.484
R_{int}	0.0193	0.0122	0.0122	0.0362	0.638 0.0146	0.579 0.0125
Refinement						
S	1.199	1.138	1.096	1.162	1.126	1.127
wR_2	0.0467	0.0257	0.0261	0.0899	0.0313	0.0269
N_{par}	184	194	200	57	238	200

Table S2. Other X-ray crystal structures of compounds discussed in this report

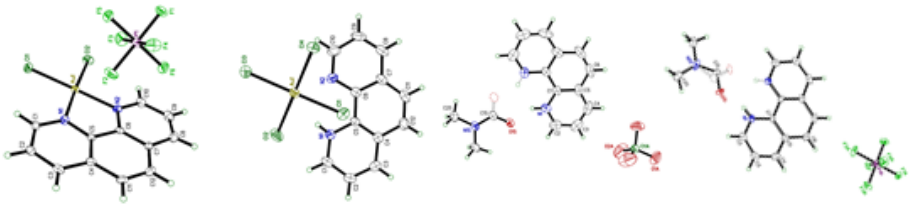

	7	H(phen)[AuCl$_4$]	H(phen)[ClO$_4$]	H(phen)[PF$_6$]
Crystal Data				
Chemical Formula	$C_{12}H_8AuCl_2F_6N_2P$	$C_{12}H_9AuCl_4N_2$	$C_{15}H_{15}ClN_3O_5$	$C_{15}H_{16}F_6N_3OP$
M_r	593.04	519.98	352.75	399.28
Crystal System	Orthorhombic	Monoclinic	Monoclinic	Orthorhombic
Space Group	*Pbca*	$P2_1/c$	$C2/c$	*Pbca*
Temperature (K)	90	180	90	90
a, b, c (Å)	12.9722(4), 15.1615(4), 15.5148(4)	7.9901(4), 7.1845(4), 25.2782(10)	10.6388(3), 22.4647(6), 6.6296(2)	11.0858(5), 22.9703(10), 6.5069(2)
α, β, γ (°)	90, 90, 90	90, 96.726(2), 90	90, 90.431(1), 90	90, 90, 90
V (Å)	3051.42(15)	1441.10(12)	1584.41(8)	1656.94(12)
Density (g/cm^3)	2.582	2.397	1.479	1.597
Z	8	4	4	4
Radiation Type	Mo Kα	Mo Kα	Mo Kα	Mo Kα
μ (mm^{-1})	10.161	10.935	0.273	0.240
F(000)	2208.0	968.0	732.0	812.0
Data Collection				
Absorption Correction	Multi-Scan	Multi-Scan	Multi-Scan	Multi-Scan
Number of Reflections	3497	3302	1827	1464
T_{min}	0.511	0.536	0.882	0.854
T_{max}	0.746	0.746	0.958	0.980
R_{int}	0.0179	0.0183	0.0404	0.0290
Refinement				
S	1.046	1.044	1.067	0.0290
wR_2	0.0326	0.0357	0.1035	0.0707
N_{par}	217	176	116	134